

Vectorized Sequence-Based Chunking for Data Deduplication

Sreeharsha Udayashankar *University of Waterloo*
 Samer Al-Kiswany *University of Waterloo*
 {s2udayas, alkiswany}@uwaterloo.ca

Abstract—Data deduplication has gained wide acclaim as a mechanism to improve storage efficiency and conserve network bandwidth. Its most critical phase, data chunking, is responsible for the overall space savings achieved via the deduplication process. However, modern data chunking algorithms are slow and compute-intensive because they scan large amounts of data while simultaneously making data-driven boundary decisions.

We present SeqCDC, a novel chunking algorithm that leverages lightweight boundary detection, content-defined skipping, and SSE/AVX acceleration to improve chunking throughput for large chunk sizes. Our evaluation shows that SeqCDC achieves $15\times$ higher throughput than unaccelerated and $1.2\times$ – $1.35\times$ higher throughput than vector-accelerated data chunking algorithms while minimally affecting deduplication space savings.

Index Terms—Data storage, Data deduplication, SIMD, Cloud computing

I. INTRODUCTION

Data generation rates have skyrocketed in recent years, leading to the explosion of the amount of data stored on the cloud [1]. Cloud storage providers employ numerous mechanisms to deal with this data influx, such as distributed file systems [2], [3], novel storage architectures [4], [5], data compression [6], [7] and data deduplication [8], [9].

Data deduplication has been widely employed in production by cloud storage providers such as Microsoft [10], EMC [11] and IBM [12]. A large percentage of the data stored by these providers is redundant [10]. Data deduplication helps identify and eliminate these redundant portions, reducing storage costs by up to 80% [11], [13]. Deduplication is performed at the *chunk-level*, after dividing files into *chunks* [14].

The division of files into chunks is achieved using data chunking algorithms [15], which dictate the space savings achieved by the deduplication system as a whole. Data chunking algorithms fall into two categories: fixed-size and content-defined chunking (CDC). Fixed-size chunking divides files into chunks of an equal pre-specified size. While this approach has been used by traditional backup systems such as Venti [13] and OceanStore [16], it achieves poor space savings due to its vulnerability to insertions and deletions that cause bytes to shift, i.e., *byte-shifting* [15].

To mitigate byte-shifting, modern deduplication systems instead resort to Content-Defined Chunking (CDC) algorithms [15], [17]–[22]. These algorithms make data-driven boundary decisions using the file’s contents, effectively handling the byte-shifting problem. Numerous data chunking algorithms are in use today and can be broadly divided into

hash-based [15], [19], [20], [22] and hashless algorithms [17], [21], [23]. Hash-based algorithms use rolling hash functions to derive chunk boundaries, while hashless algorithms treat each byte as a value and derive chunk boundaries using conditions based on local minima or maxima. Note that in either case, a *fingerprint* is generated using collision-resistant hash algorithms [24] after a chunk boundary is identified.

CDC algorithms suffer from four limitations that impact their throughput. First, they rely on expensive rolling hash functions [15], [20] and minima-maxima searches [17], [21] to determine chunk boundaries. Second, they sequentially scan the ingested data stream. This reduces throughput and increases end-to-end processing time, as real systems store terabytes of data. Third, they fail to utilize the SIMD capabilities of modern CPUs to accelerate data processing. Finally, they are designed to target datasets that benefit from smaller chunks of size 512 B – 4 KB. Such small chunks increase metadata overhead [8] and impact system throughput due to the random access and frequent transfer of small chunks.

State-of-the-art CDC techniques aimed to solve some of these shortcomings. FastCDC [19] replaced the expensive Rabin’s hash algorithm [15] with Gear hashing [20] to reduce boundary-detection overhead. AE [17] and RAM [21] reduce the overhead by avoiding hashing entirely, instead relying on minima/maxima to determine chunk boundaries. SS-CDC [18] and our previous work, VectorCDC [25], accelerate CDC algorithms with SSE/AVX instructions [26] offered by modern CPUs. However, these studies only address a few specific limitations and fail to do so effectively.

We present SeqCDC, a novel CDC algorithm that comprehensively addresses the limitations of modern CDC algorithms. SeqCDC uses three optimizations to improve chunking throughput: *lightweight boundary judgment*, *content-based data skipping*, and *vector acceleration*. Lightweight boundary judgment reduces boundary detection overhead by using monotonically increasing/decreasing sequences, avoiding complex hashing and minima-maxima searches (§III-A). To avoid scanning the entire source data, SeqCDC skips scanning selective data regions. However, to minimize the impact on deduplication efficiency, data skipping is regulated using content-based heuristics i.e. content-based skipping (§III-C). SeqCDC has been designed with vector acceleration in focus, and uses SSE/AVX instructions [26] to improve chunking throughput (§III-D). Finally, SeqCDC scales its throughput with chunk size, i.e., it offers higher throughput at the larger chunk sizes favored by deduplication systems (§VI-B).

Our evaluation compares SeqCDC to seven unaccelerated and three vector-accelerated chunking algorithms using a variety of real world datasets (§VI). We show that SeqCDC improves chunking throughput by $10\times$ over unaccelerated chunking algorithms and $1.25\times$ – $1.35\times$ over vector-accelerated CDC algorithms, while achieving comparable deduplication space savings. Our code is publicly available with DedupBench¹ [27].

II. BACKGROUND AND MOTIVATION

Data deduplication [10], [15] is used by cloud storage providers to detect duplicate data, allowing them to eliminate the costs associated with its storage and transmission. Data deduplication consists of the following steps [8]:

- *File Chunking*: Splitting a file into chunks using a data chunking algorithm is one of the primary steps in data deduplication. Deduplicating these chunks provides more space savings than file-level deduplication [15].
- *Chunk Hashing*: Each data chunk is hashed using a collision-resistant hashing algorithm, such as SHA-256 [24] or MD5 [28], to obtain a fingerprint.
- *Fingerprint Comparison*: The fingerprint is compared against a database of previously observed fingerprints. A duplicate fingerprint, i.e., one observed before, indicates an underlying duplicate chunk, which can be eliminated.
- *Data Storage*: Non-duplicate data chunks are saved on the storage medium, and their fingerprints are added to the fingerprint database.

Chunking is a critical part of this pipeline; it occurs on the critical path during data uploads and directly impacts the overall space savings and throughput associated with deduplication systems. Space savings represent the total space conserved by using deduplication.

$$\text{Space savings} = \frac{\text{Original Size} - \text{Deduplicated Size}}{\text{Original Size}} \quad (1)$$

The size of the fingerprint database is tied to the average chunk size. Smaller average sizes lead to more chunks and more fingerprints, thus increasing the size of the database and associated fingerprint comparison overheads. To minimize this overhead, deduplication systems in production tend to favor larger chunk sizes.

A. Content-Defined Chunking (CDC) Algorithms

While fixed-size chunking has been used in the past [13], it remains vulnerable to byte shifting and achieves poor space savings [15]. Content-Defined Chunking (CDC) algorithms instead make chunk boundary decisions based on the data contents. Numerous CDC algorithms [15], [17]–[23] have been proposed for data deduplication.

These algorithms slide a fixed-size window over the data within the source file. When the window’s data meets pre-specified conditions, they insert a *chunk boundary* at the end of

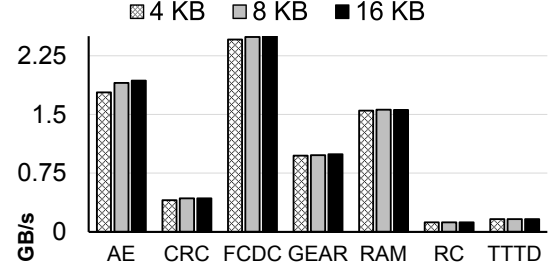


Fig. 1: Chunking throughput on randomized data

the window. By repeating this across the entire file, they divide it into data chunks. Each CDC algorithm has parameters that can be tuned to change the average size of generated chunks. CDC algorithms can be classified into hash-based and hashless algorithms [27].

Hash-based chunking algorithms, such as Rabin’s chunking [15], insert chunk boundaries only when the hash value of the window’s data matches a pre-specified mask. The hashing algorithms used here are typically not collision-resistant. For instance, with Rabin’s Chunking (RC) [15], chunk boundaries are inserted when the lower order 13 bits of the hash value are zero. While Rabin’s chunking achieves high deduplication ratios, it is very slow. TTTD [22] uses Rabin’s hashing but improves space savings by simultaneously checking for two hash value conditions. The secondary condition is always computed but only used if a boundary is not found beyond a pre-specified size with the primary condition.

The CRC [18] and Gear [20] hashing functions have lower overheads than Rabin’s hashing. FastCDC (FCDC) [19] uses Gear hashing and implements two optimizations to improve chunking throughput: sub-minimum skipping and chunk size normalization. Sub-minimum skipping skips scanning data up to the minimum chunk size at the beginning of each chunk. Chunk size normalization dynamically relaxes the boundary condition to ensure that generated chunks are close to the expected average chunk size.

Hashless algorithms such as Asymmetric Extremum (AE) [17] and Rapid Asymmetric Maximum (RAM) [21] also slide fixed-size windows over the source data. AE attempts to identify a window such that the starting byte’s value is greater than all the bytes before it and not less than the other bytes within the window. When such a window is found, AE inserts a chunk boundary at the end of the window. AE is 4 – $5\times$ faster than Rabin’s chunking. Rapid Asymmetric Maximum [21] inserts chunk boundaries when the byte immediately outside the window has a value greater than the maximum-valued byte within the window. These algorithms avoid hashing when determining chunk boundaries, reducing boundary-detection overhead and achieving high chunking throughput [25], [29].

B. Chunking Throughput Analysis

As noted above, deduplication systems in production prefer a smaller number of larger size chunks, to minimize fingerprinting overheads. However, state-of-the-art CDC algorithms are designed with smaller chunk sizes in mind i.e., their throughput remains constant across chunk sizes.

¹<https://github.com/UWASL/dedup-bench>

Figure 1 shows the throughput achieved by AE [17], CRC [18], FastCDC (FCDC) [19], Gear-based chunking [20], RAM [21], Rabin’s Chunking (RC) [15] and TTTD [22] when chunking a 1GB file containing random data. We compare the chunking throughput of these algorithms across three average chunk sizes: 4 KB, 8 KB, and 16 KB. This experiment was run on a machine with an Intel Icelake CPU, the details of which are in §VI.

We note that the throughputs of all these algorithms do not scale with chunk size, as they process the entire data stream regardless of target size. One of the motivating factors behind SeqCDC was to achieve higher throughput at larger chunk sizes used in production.

When targeting larger chunk sizes, most of the scanned data does not qualify as chunk boundaries. To minimize wasteful computation at larger chunk sizes, we propose skipping data regions during scanning. As random skipping can severely degrade the space savings achieved by deduplication, we use *content-defined data skipping* to skip scanning only certain regions (§III-C) using data-based heuristics. At larger chunk sizes, SeqCDC can afford to skip larger amounts of data without impacting space savings, leading to higher throughput.

C. Accelerating CDC algorithms with vector instructions

Vector instruction sets [26] are supported by most modern Intel and AMD CPUs. These instructions allow for the execution of arithmetic/logical operations simultaneously on multiple pieces of data, i.e., the *Single-Instruction Multiple-Data (SIMD)* paradigm. To do this, they rely on special vector registers provided within the CPU, packing multiple values into them and operating on all the values with a single operation such as an addition or subtraction. Depending on the amount of data they process at once, these instructions can be classified as SSE-128, AVX-256, and AVX-512, i.e., 128-bit, 256-bit, or 512-bit. While AVX-512 instructions are only supported by the newest Intel and AMD CPUs, SSE-128 and AVX-256 support has been available since 2003 and 2011, respectively.

Vector instructions have previously been used to accelerate mathematical operations [30], [31] and multimedia applications [32]. SS-CDC [18] previously attempted to accelerate hash-based CDC algorithms, such as CRC-32 and Gear [20], using AVX-512 instructions. They decouple the rolling hash and boundary detection phases to accelerate them separately. However, many hash-based algorithms such as FastCDC [19] and TTTD [33] use minimum chunk size skipping to improve throughput. Running the rolling hash phase on the entire source data and identifying boundaries later in a separate phase eliminates this throughput benefit. Additionally, due to the dependency between adjacent bytes when calculating hash values, accelerating rolling hash algorithms is complicated. To solve this, SS-CDC resorted to processing different regions of the data simultaneously with AVX-512 instructions, i.e., rolling with multiple heads. As this requires expensive vector scatter/gather instructions, the speedups achieved are limited, as shown by our previous work VectorCDC [25].

VectorCDC [25] instead accelerates hashless algorithms such as AE [17] and RAM [21] with vector instructions. It

identifies two phases common to these algorithms, the *Extreme Byte Search* and *Range Scan* phases, accelerating them using different vector-based techniques. Using these techniques, VectorCDC [25] achieved orders of magnitude higher speedup for hashless algorithms than what SS-CDC [18] achieved for hash-based ones. While beneficial, vector-acceleration alone cannot improve chunking throughput at larger sizes (§VI-B).

Despite being hashless, SeqCDC does not follow the same paradigm as AE and RAM. SeqCDC uses content-defined skipping (§III-C). Additionally, instead of relying on minimum/maximum byte values to detect chunk boundaries, SeqCDC uses monotonically increasing/decreasing sequences (§III). Thus, VectorCDC’s approach is incompatible with SeqCDC.

III. SEQCDC’S DESIGN

SeqCDC is designed to insert chunk boundaries when fixed-length sequences of monotonically increasing/decreasing bytes are detected. SeqCDC can operate in either *Increasing* mode i.e. targeting increasing order sequences or *Decreasing* mode. Note that these two modes are exclusive of each other. Figure 2 shows an example of SeqCDC’s operation. §IV discusses how SeqCDC is resistant to byte shifting.

SeqCDC utilizes three parameters: *SeqLength*, *SkipTrigger* and *SkipSize*, each described in detail in the following subsections. SeqCDC includes four optimizations we discuss in detail: lightweight boundary detection, ignoring data at the beginning of a chunk, content-based data skipping, and acceleration with vector instructions.

A. Lightweight Boundary Detection

To avoid complex hashing operations, SeqCDC treats each byte within the data stream as an independent value similar to existing hashless CDC algorithms [17], [21]. However, to improve chunking throughput even further, SeqCDC reduces the overheads associated with boundary detection by avoiding minima/maxima searches.

Instead, SeqCDC looks for *fixed-length monotonically increasing/decreasing* sequences of bytes and inserts chunk boundaries whenever such a sequence is detected. The sequence must have a length of *SeqLength* to be considered a boundary candidate. Once such a sequence is found, a boundary is inserted at its end.

Modes of operation. SeqCDC can be used in *Increasing* or *Decreasing* mode. Both these modes are exclusive of each other. While in *Increasing* mode, SeqCDC targets monotonically increasing sequences. On the other hand, it targets monotonically decreasing sequences in *Decreasing* mode. Depending upon dataset characteristics, one mode may be more effective than the other.

Figure 2 shows an example of SeqCDC operating in *Increasing* mode with a *SeqLength* of 3. A chunk boundary is inserted after the byte with value 98, as it forms an increasing sequence with the bytes preceding it.

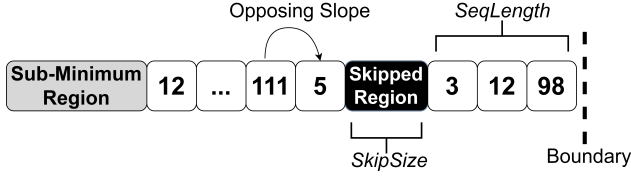


Fig. 2: An example of a chunk generated by SeqCDC

B. Ignoring Sub-minimum Regions

SeqCDC utilizes the concept of ignoring data at the beginning of each chunk introduced within previous literature [19], [33] to increase chunking throughput. SeqCDC skips scanning data of size $(\text{minimum_chunk_size} - \text{SeqLength})$ at the beginning of each chunk ("Sub Minimum Region" in Figure 2).

Increasing the minimum chunk size allows SeqCDC to skip over larger amounts of data at the beginning of each chunk, increasing chunking throughput. However, when performed excessively, this may negatively impact space savings on some datasets. The minimum chunk size for SeqCDC is 25-50% the average chunk size, similar to existing algorithms [19], [33].

C. Content-based Data Skipping

SeqCDC additionally improves chunking throughput by skipping scanning certain data regions when looking for chunk boundaries ("Skipped Region" in Figure 2). Randomly skipping data regions can lead to missed boundaries, lowering byte-shifting resistance and negatively affecting space savings. To avoid this, SeqCDC adopts a novel content-based data skipping mechanism, i.e., data regions are skipped over only when skip conditions are met.

SeqCDC skips scanning data within *unfavorable regions*, i.e., data regions with byte sequences in an order opposing the target sequence. For instance, when in *Increasing* mode, regions with decreasing order sequences are considered unfavorable. When *SkipTrigger* pairs of bytes in opposing order are detected, SeqCDC decides that the current region is unfavorable and skips scanning the next few bytes in the hope of landing in a favorable region, with bytes in the chosen order. For instance, in Figure 2, the skip condition is triggered after the byte with a value of 5, causing the next *SkipSize* bytes to be ignored. The *SkipSize* is kept small at 256-512 bytes, to avoid skipping over large sections of data. After a skip is triggered, SeqCDC resets its counters and resumes scanning for boundaries.

Larger *SkipSizes* improve chunking throughput. While larger *SkipSizes* are feasible for larger chunks, they may result in a disproportionately high amount of data skipped within smaller chunks, negatively affecting space savings. SeqCDC overcomes this by adjusting the *SkipSize* from 256–512 bytes, depending on the expected average chunk size.

Data skipping can potentially impact byte-shifting resistance. SeqCDC therefore trades off a small reduction in space savings for higher chunking throughput. Section IV discusses this trade-off in greater detail. Additionally, in our evaluation

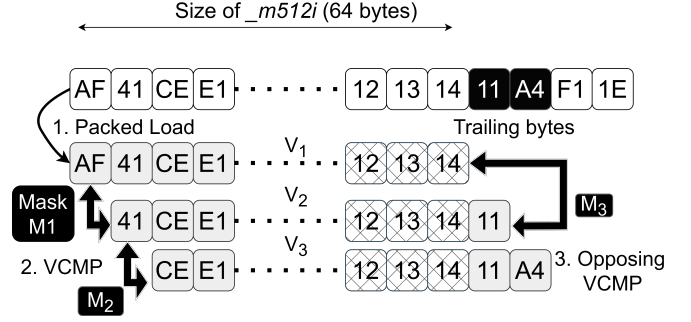


Fig. 3: Accelerating SeqCDC with AVX-512 instructions

(§VI-A), we show that this design decision minimally impacts space savings in real datasets.

D. Accelerating SeqCDC with vector instructions

VectorCDC [25] demonstrated the throughput benefits that can be obtained by using vector instructions to accelerate data chunking algorithms. However, VectorCDC's approach cannot be directly applied to accelerate SeqCDC (§II-C), as SeqCDC relies on detecting monotonically increasing/decreasing sequences for chunk boundaries. We propose an alternate vector-based method to accelerate SeqCDC in this section.

Figure 3 shows an example of accelerating SeqCDC operating with a *SeqLength* of 3 and *Increasing* mode using AVX-512 instructions [26]. The figure shows a byte range with byte values AF–1E that need to be scanned for boundaries. A chunk boundary sequence starting at byte 12 exists in this region and is shown with a cross-stitched pattern. Let us assume scanning begins at byte AF.

Scan Procedure. We start by loading the 64 bytes AF–14 into a vector register V_1 in packed fashion (Step 1). We then load bytes at an offset of 1 from this position, i.e., 41–11 into another vector register V_2 . We repeat this process for a total of *SeqLength* vector registers, i.e., until V_3 in this case.

In Step 2, we run a vector comparison operation `mm512_cmpgt` between V_2 and V_1 . This operation compares pairwise bytes in both registers to see if the byte from V_2 is greater than its counterpart from V_1 . For instance, byte 41 from V_2 is compared against byte AF from V_1 as they are both the first bytes in their respective registers. The operation generates a 64-bit mask M_1 , containing set bits for all positions where the byte from V_2 is greater than that of V_1 . We repeat this operation between registers V_3 and V_2 as well to generate mask M_2 .

In Step 3, we run a single vector comparison operation between registers V_2 and V_1 . This is a `mm512_cmplt`, which compares pairwise bytes, checking for bytes in V_2 *lesser* than those in V_1 . The operation generates a bit mask M_3 . Note that this is an opposite comparison operation to Step 2.

Following this, we check for boundaries and opposing byte pairs (detailed below) before moving the scan position by 64 bytes, i.e., to byte 11. Effectively, we are scanning for chunk boundaries and content-defined skips 64 bytes at a time. Finally, note that while trailing bytes 11 and A4 are used in Steps 1 and 2, we have not scanned for boundary sequences

beginning at these bytes yet. Thus, they are used again when scanning moves ahead.

Boundary Detection. To detect boundaries, we use the masks obtained in Step 2. Each of these masks contains set bits corresponding to increasing byte pairs. If we combine all the masks using a bitwise AND operation, the resulting mask only contains set bits in positions with increasing bytes from all pairwise vector comparisons. If a bit at index k is set within M_1 , it indicates that the byte at index k in V_2 is greater than the one at index k from V_1 . Similarly, a set bit index k in M_2 indicates that the byte at index k in V_3 is greater than the byte at index k from V_2 .

For instance, in Figure 3, the bit at index 61 in mask M_1 represents a comparison between byte 13 from V_2 and byte 12 from V_1 and will have a set bit. Similarly, the bit with index 61 in M_2 will be set as it compares byte 14 from V_3 with byte 13 from V_2 . Thus, the resulting mask obtained using $M_1 \& M_2$ will have a set bit at index 61.

Boundaries can be detected by examining the resulting combined mask $M_1 \& M_2$. If the mask contains any set bits (has a non-zero value), a chunk boundary is declared at *SeqLength* bytes ahead of the first set bit's position.

Content-defined skipping. To detect opposing pairs of bytes, we use mask M_3 obtained in Step 3. This mask contains set bits at all positions where a byte from V_2 is lesser than its counterpart from V_1 . Thus, the total opposing byte pairs observed in the current scanned region equals the number of set bits in M_3 . We keep a running total of the number of these opposing byte pairs. When the running total exceeds *SkipTrigger*, a content-defined skip of *SkipSize* bytes is initiated as described in §III-C. The exact position to jump from is determined using the first set bit that causes the total to exceed *SkipTrigger*.

Accelerated x86 Intrinsics. Intel and AMD CPUs support many other hardware-accelerated intrinsics. Forward Scan (*builtin_ffs*) is used to find the first set bit in 32/64-bit integers. Parallel Bit Deposit (*pdep*) is used to deposit contiguous low bits into a destination integer. Trailing Zero Count (*tzcnt*) is used to count the number of trailing zeros in an integer. Population Count (*popcnt*) is used to count the number of set bits in an integer. While these are hardware accelerated, they fall under other CPU instruction sets i.e., they are not vector instructions.

Boundary detection needs to identify the first set bit in a mask, while content-defined skips need to identify the first set bit that causes the running total to exceed *SkipTrigger*, i.e., the n^{th} set bit. We use hardware-accelerated x86 intrinsics [34] for both of these; *builtin_ffs* for boundary detection, and a combination of *pdep* and *tzcnt* for content-defined skipping. In addition, we use *popcnt* within content-defined skipping to count the total number of set bits in the opposing slope mask. Note that the performance of these intrinsics varies across CPU architectures.

IV. IMPACT OF INSERTIONS AND DELETIONS

Inserting or deleting bytes from the middle of a file causes the data bytes to shift, resulting in changes to certain chunk

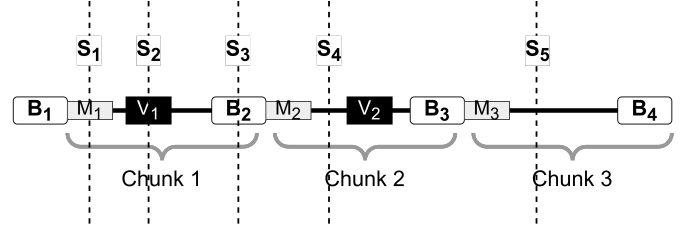


Fig. 4: Handling byte-shifts with SeqCDC

boundaries. Byte shifting can span one or more bytes and take the form of insertions or deletions. In general, sub-minimum and content-defined skipped regions affect SeqCDC's byte-shifting resistance. Figure 4 shows three chunks with four boundary sequences $B_1 - B_4$. Each chunk has a corresponding sub-minimum region ($M_1 - M_3$) at the beginning of the chunk. The figure also shows two regions V_1 and V_2 skipped via SeqCDC's content-defined skipping i.e., using *SkipTrigger*, and five byte shifts $S_1 - S_5$.

Skipped region impact: When byte-shifts occur, boundaries may be moved in and out of skipped regions (both sub-minimum and content-defined). This occurs with large byte-shifts when boundaries are close to these regions. For instance, consider S_1 in Figure 4 which occurs in the sub-minimum region M_1 . If byte-shift S_1 causes a boundary previously hidden within M_1 to be pushed outside, a new chunk may be created, thus splitting Chunk 1. This may in turn lead B_2 to be pushed into M_2 , affecting a few subsequent chunks as well. Similarly, a deletion may cause B_2 to be hidden within M_1 , leading to chunk mergers. Additionally, boundaries may be moved in and out of regions previously skipped with *SkipTrigger* and *SkipSize* by shifts such as S_2 , causing chunk splits and mergers.

While this behavior can theoretically impact a large number of chunks, it only impacts a limited number of chunks within real datasets. This is why many CDC algorithms, such as FastCDC [19] and TTTD [33] use sub-minimum skips in production. SeqCDC also minimizes the impact caused by content-defined skipping by keeping the *SkipSize* between 256-512 bytes. Thus, despite data skipping, SeqCDC achieves competitive space savings with other CDC algorithms, as shown in §VI-A. Finally, we note that all CDC algorithms have pathological data patterns i.e. data engineered to ensure that they are ineffective.

In the rest of this section, we focus on the more common kind of byte-shifting i.e. those that do not result in new boundaries being uncovered or hidden, simply being shifted instead.

Within the boundary sequence. The probability of byte shifting occurring within a boundary sequence is rare in real datasets, as *SeqLength* typically ranges from 3 to 7 bytes. If byte shifting occurs within a sequence, the boundary may no longer exist. Thus, scanning will continue until the next sequence is detected. In Figure 4, S_3 may cause B_2 to no longer exist. Thus, the next boundary will be after B_3 , causing Chunks 1 and 2 to be merged while subsequent chunks are unaffected.

	<i>SeqLength</i>	<i>SkipTrigger</i>	<i>SkipSize</i>
4 KB	5	55	256
8 KB	5	50	256
16 KB	5	50	512

TABLE I: SeqCDC parameter values

Between sequences and outside skipped regions. Byte-shifts such as S_4 are the ones most commonly seen in real datasets. They occur outside of skipped regions and do not drastically change the chunk structure. If S_4 does not create a new boundary sequence, the existing boundary sequence B_3 shifts. Thus, Chunk 2 changes while subsequent chunks are unaffected. On the other hand, if S_4 does create a new boundary sequence, a boundary is inserted after it, changing Chunk 2. Depending on the shift position, the next boundary detected may be B_3 or B_4 , resulting in a changed Chunk 3 as well. Thus, Chunks 2 and 3 are affected while others are unaffected.

Maximum chunk size. If a shift S_5 causes the maximum chunk size to be reached, a boundary is inserted at the maximum chunk size similar to existing algorithms [17], [19], [21]. This will cause the chunk to split into multiple chunks. For instance, if a boundary is inserted after S_5 in Figure 4, Chunk 3 will be split into two if no subsequent boundary sequences are hidden.

V. IMPLEMENTATION

We implemented a native (unaccelerated) version of SeqCDC using approximately 250 lines of C++ code. We optimized the computation of *SeqLength* and *SkipTrigger* using the `std::signbit` function to reduce the number of branch conditions. We have released this code publicly with Dedup-Bench [27].

We implemented the vector acceleration described in §III-D using an additional 350 lines of C++ code. We have implemented SSE-128, AVX-256 and AVX-512 compatible accelerations for SeqCDC. SeqCDC is compatible with all file and data formats.

Obtaining parameter values. SeqCDC has three configurable parameters apart from its mode: *SeqLength*, *SkipTrigger* and *SkipSize*. To obtain the parameter value combination needed to generate a given average chunk size, we first used Monte-Carlo simulations [35] on randomized data streams. For example, to identify the parameter values for an average of 4 KB, we conducted simulations on randomized data to identify candidate combinations resulting in an average chunk size of 4 KB. Following this, we experimented on one of our datasets (DEB from §VI) to pick the best performing combination, which we use across all the datasets in our evaluation. The final values used within our evaluation (§VI) for average chunk sizes of 4-16 KB are shown in Table I.

The results outlined in §VI show that SeqCDC outperforms other CDC algorithms on all datasets with these chosen parameters. Thus, it is not necessary to run an extensive parameter search per dataset, instead obtaining suitable parameters using the method described above. However, to tune SeqCDC to

Dataset	Size	Information	XC
DEB	40 GB	65 Debian VM Images from VMware Marketplace [36]	18.98%
DEV	230 GB	100 backups of a Rust [37] nightly build server	83.17%
LNK	65 GB	160 Linux kernel distributions in TAR format [38]	19.87%
RDS	122 GB	100 Redis [39] snapshots with <code>redis-benchmark</code> runs	33.54%
TPCC	106 GB	25 snapshots of a MySQL [40] VM running TPC-C [41].	37.39%

TABLE II: Dataset information. Note that XC is the space savings achieved using 8 KB fixed-size chunks.

a specific dataset, better parameter combinations may be obtained using such a search.

x86 intrinsics performance. As noted in §III-D, the performance of `popcnt`, `pdep` and `tzcnt` may vary across CPU architectures. In order to estimate their performance on a given CPU, we implemented an x86 intrinsics micro benchmark using approximately 250 lines of C++ code. We will release this micro benchmark with the final version of our paper.

VI. EVALUATION

In this section, we evaluate SeqCDC’s space savings, chunk size distribution, and chunking throughput and compare it to the state-of-the-art CDC algorithms.

Testbed. We use machines with Intel Skylake and Icelake CPUs from CloudLab Wisconsin [42] for our evaluation. The Skylake machine (*c220g5*) consists of two 10-core Intel Xeon Silver 4114 CPUs with hyperthreading, 192 GB of RAM, and a 10 GBps Intel NIC. The Icelake machine (*sm220u*) consists of two 16-core Intel Xeon Silver 4314 CPUs with hyperthreading, 256 GB of RAM and a 100 GBps Mellanox NIC. Unless otherwise mentioned, we show results from the Icelake machine. All our results are the average of 5 runs with a standard deviation of less than 5%.

Alternatives. We evaluate the following hash-based CDC algorithms:

- **CRC:** A hash-based chunking algorithm using CRC-32 [18].
- **FCDC:** FastCDC [19] with a normalization level of 2.
- **GEAR:** Gear-based chunking [20].
- **RC:** A hash-based CDC using Rabin’s fingerprinting algorithm [15].
- **SS-CRC:** AVX-512 version of CRC, accelerated with SS-CDC [18].
- **SS-Gear:** AVX-512 version of Gear, accelerated with SS-CDC [18].
- **TTTD:** Two-Threshold Two-Divisor Algorithm, based on Rabin’s fingerprinting with a backup divisor [22].

We also evaluate the following hashless CDC algorithms:

- **AE:** The Asymmetric Extremum [17] algorithm.
- **RAM:** Rapid Asymmetric Maximum [21].
- **VRAM:** SSE-128, AVX-256, and AVX-512 versions of RAM accelerated with VectorCDC [25].

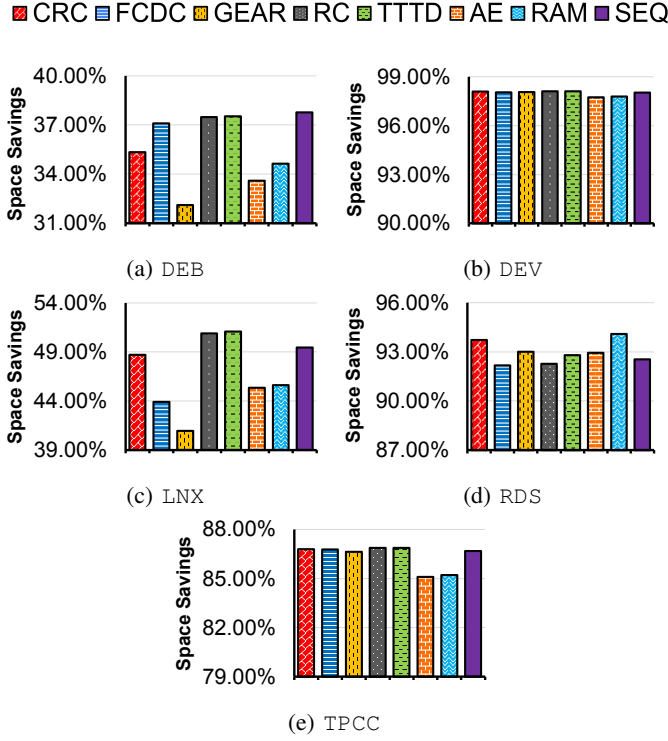


Fig. 5: Space Savings with 8KB chunks. Note that *SEQ* is unaccelerated SeqCDC.

- *SEQ*: Native version of SeqCDC. We only report the results for SeqCDC in *Increasing* mode. The results for *Decreasing* mode are similar.
- *VSEQ*: SSE-128, AVX-256, and AVX-512 versions of SeqCDC in *Increasing* mode.

We use minimum and maximum chunk sizes of $\frac{1}{2} \times$ and $2 \times$ the expected average chunk size, in line with previous studies [19], [33]. The only exception is that for a small average chunk size of 4 KB, we use a minimum size of 1 KB.

Datasets. Table II shows the datasets used in our evaluation as well as the space savings achieved by using fixed-size chunking (XC) with an average size of 8 KB. The datasets represent diverse workloads such as database backups, VMs, and Linux kernel code. We have made the DEB dataset publicly available² [43].

A. Space Savings

Figure 5 shows the space savings achieved by all the alternatives across datasets with 8 KB chunks. By comparing the space savings achieved by fixed-size chunking (XC) on all datasets (Table II) to those achieved by the CDC algorithms (Figure 5), we note that CDC algorithms achieve superior space savings to XC. For instance, XC achieves a space savings of only 37.39% on TPCC, while CDC algorithms achieve 86–87%. The detailed results for all chunk sizes, algorithms, and dataset combinations are in the Appendix in Table III.

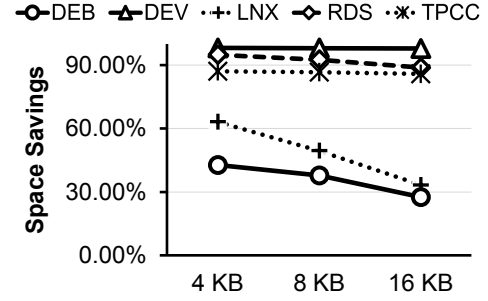


Fig. 6: SeqCDC's Space Savings vs Chunk Size across datasets

CDC comparison. From Figure 5, we see that SeqCDC (*SEQ*) achieves similar space savings to all the other CDC algorithms on these datasets with 8 KB chunks. The best algorithm for space savings varies depending on the dataset. For instance, *TTTD*, *RAM*, and *SEQ* achieve the best space savings on DEV, RDS, and TPCC respectively. The detailed results for all chunk sizes are in the Appendix in Table III. On all datasets, SeqCDC either is the best or achieves space savings within 6% of the best performer for all chunk sizes.

Dataset characteristics. Figure 6 shows the space savings variation across chunk sizes for all our datasets using SeqCDC; the results are similar for other CDC algorithms. The space savings achieved decrease with increasing chunk size across datasets.

The space savings degradation between 4 KB and 16 KB average chunk sizes on the DEV, RDS, and TPCC datasets is 0.5–6%. However, as the total number of chunks at 16 KB is far lower than that at 4 KB, the size of the fingerprint database and fingerprinting overheads are significantly lower. Similarly, the best chunk size configuration for the DEB dataset is 8 KB. This demonstrates why deduplication systems favor larger chunk sizes on some datasets.

On the other hand, the LNX dataset presents a case favoring smaller chunk sizes. The space savings degradation for LNX in Figure 6 moving from average chunk sizes of 4 KB to 16 KB is 29.87%. This far outweighs any gains within fingerprint indexing.

Vector acceleration. We observed that vector acceleration minimally impacts the space savings achieved by CDC algorithms, in line with previously observed results [18], [25]. For instance, *SS-CRC* and *CRC* achieve the same space savings values. We have excluded these results from Figure 5 for clarity. Similarly, vector acceleration does not impact SeqCDC's space savings.

B. Chunking Throughput: Unaccelerated CDC

Figure 7 shows the chunking throughput for all unaccelerated CDC algorithms on DEB and TPCC. The results for other datasets are similar. When examining chunking throughputs across average chunk sizes, we note that the throughput minimally scales with size for all algorithms other than *SEQ*, similar to our analysis in §II-B.

Among the hash-based algorithms, *RC* [15] and *TTTD* [22] are the slowest, only achieving 0.12 – 0.22 GB/s. *TTTD* is

²<https://www.kaggle.com/datasets/sreeharshau/vm-deb-fast25>

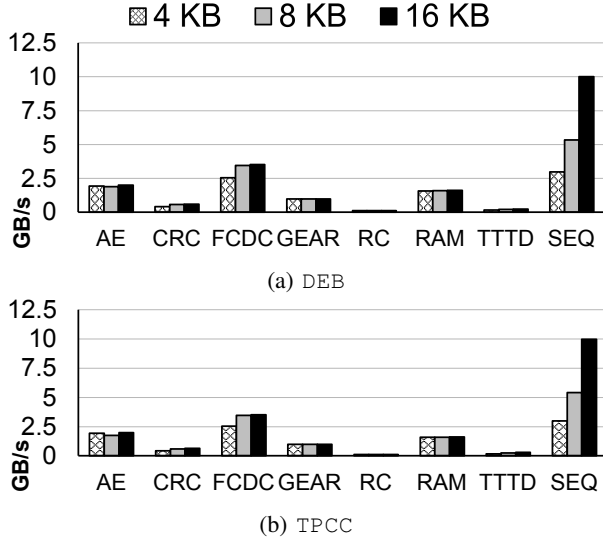


Fig. 7: Chunking throughput of native CDC algorithms. Note that *SEQ* is unaccelerated SeqCDC.

slightly faster than Rabin’s chunking due to sub-minimum skipping (§II-A). The poor chunking throughput of both algorithms is due to the high computational cost of Rabin’s hashing, as pointed out in previous literature [19]. *GEAR* chunking [20] uses the faster gear hash algorithm allowing it to reach 0.95 – 0.98 GB/s. FastCDC (*FCDC*) fares significantly better and achieves 2.5 – 3.5 GB/s, largely due to sub-minimum skipping and using the Gear hashing algorithm. *FCDC*’s throughput increases between average chunk sizes of 4 KB to 8 KB due to the increased ratio of the sub-minimum region size to chunk size (25% to 50%).

Hashless algorithms such as *AE* [17] and *RAM* [21] achieve higher chunking throughput than all hash-based algorithms except *FCDC*. They both achieve throughputs of 1.5–1.9 GB/s across datasets.

Unaccelerated SeqCDC (*SEQ*) consistently achieves higher chunking throughput than all other CDC algorithms at average chunk sizes of 8 KB and 16 KB. At a chunk size of 8 KB, it achieves 5.3 – 5.4 GB/s, 1.5× and 2.8× better than *FCDC* and *AE* respectively. At a chunk size of 16 KB, it achieves a chunking throughput of 9.9 – 10 GB/s, 2.8× and 5.2× better than *FCDC* and *AE* respectively. *SEQ*’s increase in throughput from 8 KB to 16 KB is primarily due to the increasing *SkipSize* from 256 bytes to 512 bytes.

At a chunk size of 4 KB, SeqCDC’s *SkipTrigger* is increased by 10% to constrain the amount of data skipped. SeqCDC still achieves 2.9 GB/s, 1.16× and 1.5× faster than *FCDC* and *AE* respectively. Thus, *native SeqCDC is faster than other native CDC algorithms by 1.5×–2.8× at larger chunk sizes and 16% at smaller chunk sizes.*

C. Chunking Throughput: Vector-accelerated CDC

Figure 8 shows the throughput of native algorithms with their respective AVX-512 accelerated versions; *CRC* and *Gear* accelerated with SS-CDC [18], *RAM* accelerated with Vector-CDC [25] and SeqCDC accelerated with the method described

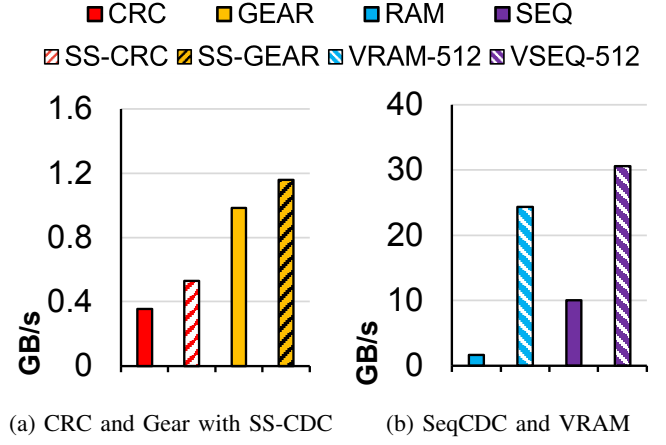


Fig. 8: Chunking speedups on DEB with 16 KB chunks

in §III-D. Figure 8b shows that *VSEQ-512* achieves the highest throughput among all vector-accelerated algorithms, at 30.5 GB/s. It is also 10× faster than *FCDC*, the fastest non-vector alternative.

Vector speedups. *SS-CRC* and *SS-Gear* (Figure 8a) achieve low speedups over their native counterparts due to using scatter / gather instructions and dependencies between adjacent bytes (§II-C). Hashless vector-based algorithms such as *VRAM* and *VSEQ* do not suffer from these limitations. It is important to note that while *VSEQ* achieves the highest throughput overall, its speedup over its native counterpart is lower than that of *VRAM* (Figure 8b). *VSEQ-512* achieves a 3.05× speedup over *SEQ* while *VRAM-512* achieves a 16× speedup over *RAM*. Thus, *SeqCDC is not as vector friendly as RAM.*

For the rest of our evaluation, we will use only *VSEQ* and *VRAM*.

VSEQ vs VRAM. Figure 9 compares the two best performing alternatives *VSEQ-512* and *VRAM-512* across different chunk sizes on DEB and TPCC. The figure shows that *VRAM* cannot scale its throughput with increasing chunk sizes, similar to its native counterpart *RAM*. Thus, *vector-acceleration alone cannot fix the inability of CDC algorithms to scale their throughput with chunk size.* *VSEQ* can accomplish this due to its changing *SkipSize*, similar to *SEQ*.

At lower chunk sizes such as 4 KB, we note that *VRAM* outperforms *VSEQ*. However, at 8 KB this performance gap quickly closes. At 16 KB, *VSEQ* outperforms *VRAM* by 1.23 – 1.35×. This gap increases further at larger chunk sizes. Thus, while *VRAM* is faster at smaller chunk sizes, *VSEQ is 1.23 – 1.35× faster than VRAM at the larger chunk sizes favored by deduplication systems.*

Throughput breakdown. Figure 10 shows the impact of each optimization (§III) on SeqCDC’s throughput. We use 16 KB chunks for this experiment.

BASE represents native SeqCDC running with only lightweight boundary judgement and sub-minimum skipping i.e. without content-defined skipping. *SEQ* enables content-defined skipping. *VBASE-512* represent an AVX-512 accelerated SeqCDC without content-defined skipping. Finally *VSEQ-512* uses both AVX-512 acceleration and content-defined skips.

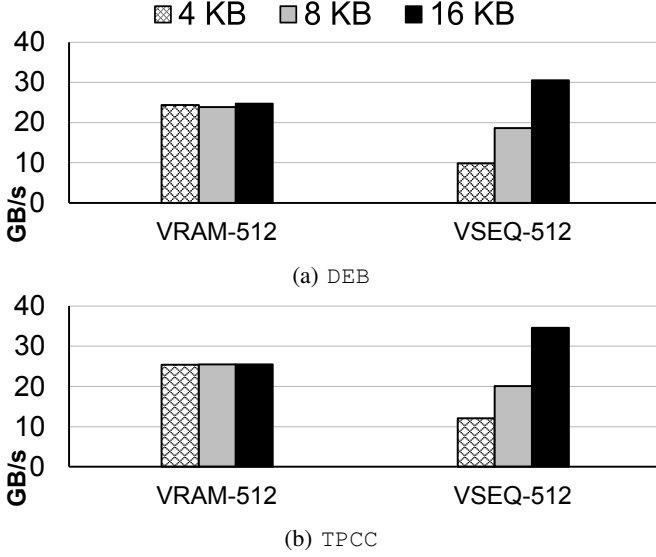


Fig. 9: Chunking throughput of vector accelerated CDC algorithms. Note that *VSEQ* is vector accelerated SeqCDC.

We note that content-defined skipping is beneficial on all datasets without AVX-512 acceleration, albeit to different extents. For instance, content-defined skipping allows *SEQ* to achieve $2.2\times$ – $2.6\times$ higher throughput than *BASE* on LNX and RDS. On the other hand, it only achieves $1.38\times$ on DEB.

When pairing content-defined skips with AVX-512 acceleration, the landscape changes. We notice three kinds of behavior between *VBASE-512* and *VSEQ-512* in Figure 10. On RDS, the benefits are still significant, with *VSEQ-512* achieving a $2.61\times$ higher throughput than *VBASE-512*. On DEV, LNX, and TPCC, the speedups are slightly lower at $1.12\times$ – $1.41\times$. Finally, on DEB, skipping is not beneficial.

Despite being hardware-accelerated, keeping track of opposing slopes and jump positions does not require vector instructions; it uses Bit Manipulation Instructions (BMI and BMI-2) [44]. Such intermingling of vectorized and non-vectorized code regions leads to lower performance gains [45], and may outweigh the benefits of content-defined skips on certain datasets. Thus, while SeqCDC’s *content-defined skipping* is almost always beneficial without vector instructions, its benefits depend on dataset characteristics when paired with vector instructions.

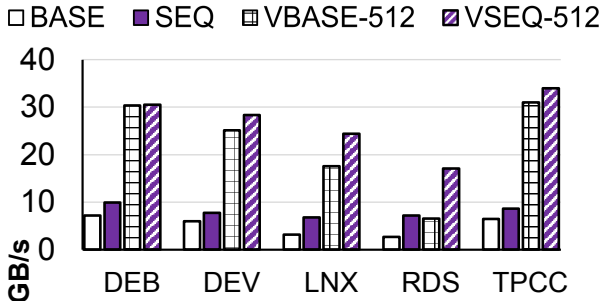


Fig. 10: SeqCDC’s throughput breakdown at 16 KB with native and AVX-512 instructions

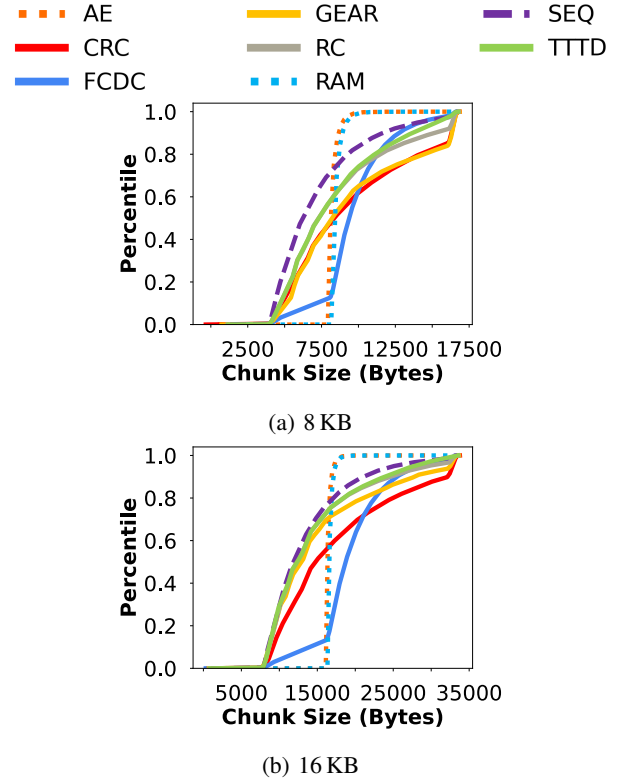


Fig. 11: Chunk size distribution (CDF) on TPCC

D. Backward compatibility with AVX-256 and SSE-128

Only a handful number of newer Intel and AMD processors support AVX-512 instructions. However, SSE-128 and AVX-256 instructions have been supported by Intel and AMD since 2003 and 2011 respectively. Thus, most CPUs available today support one of the three classes of vector instructions.

While SeqCDC’s design described in §III-D uses AVX-512 instructions, SeqCDC can be accelerated with SSE-128/AVX-256 instructions as well. Figures 12a and 12c show the benefits of accelerating SeqCDC with SSE-128, AVX-256, and AVX-512 instructions on two different CPU architectures: Intel Skylake and Intel Icelake. We use the DEB dataset.

We note that *VSEQ-128* and *VSEQ-256* achieve significant speedups over *SEQ* on both architectures. For instance with 16 KB chunks, *VSEQ-128* achieves a $1.57\times$ – $2.19\times$ speedup on both architectures. Similarly, *VSEQ-256* at 16 KB achieves a $2.52\times$ – $3.34\times$ speedup. Thus, SeqCDC retains most of its throughput benefits when accelerated with SSE-128 and AVX-256 instructions, and is compatible with most modern CPUs.

Note that the speedups slightly vary across architectures. For instance, *VSEQ-512* achieves a $5.8\times$ speedup over *SEQ* on the Skylake while it achieves $3.05\times$ on the Icelake machine. This is largely tied to CPU microarchitecture and x86 intrinsic performance as described in §III-D.

SeqCDC vs VRAM. Figures 12b and 12d compare *VSEQ* with the best performing vector accelerated alternative, *VRAM*, using SSE-128, AVX-256 and AVX-512 instructions on Intel Skylake and Icelake architectures. We use DEB with 16 KB chunks for this experiment. We see that *VSEQ* maintains its performance advantage over *VRAM* with all vector instruction

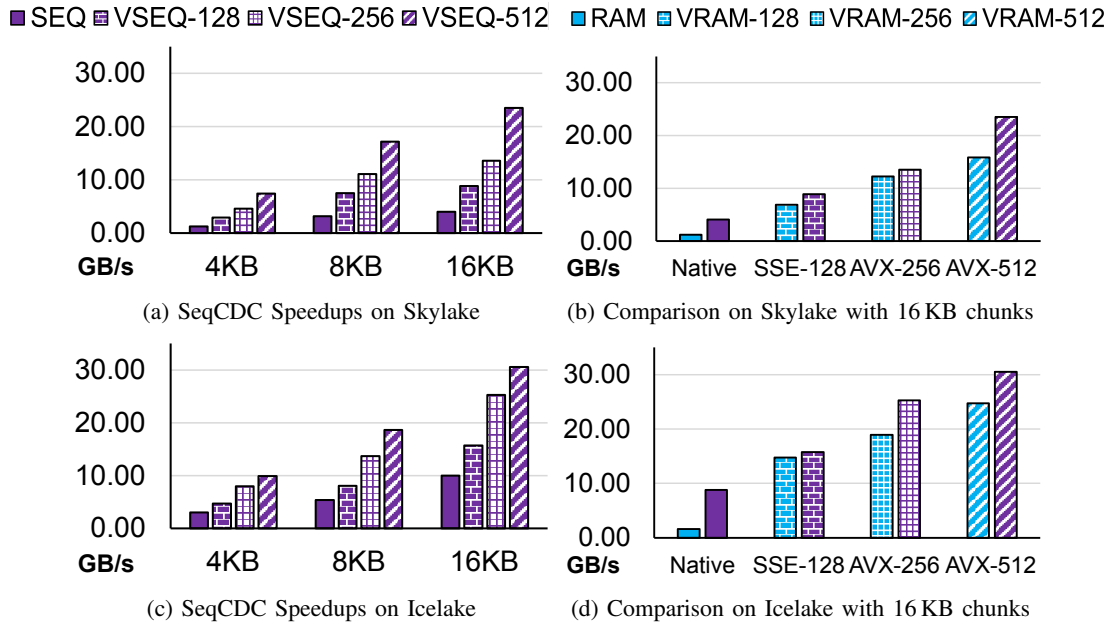


Fig. 12: Chunking Throughput on DEB with SSE-128, AVX-256 and AVX-512 Instructions

families, further cementing its effectiveness and backward compatibility.

E. Chunk Size Distribution

CDC algorithms are expected to achieve a uniform chunk size distribution, loosely centered around the average chunk size. Figure 11 shows a CDF of chunk sizes from all algorithms on the TPCC dataset at average sizes of 8 KB and 16 KB. Hash-based algorithms' distributions are shown using solid lines, while hashless algorithms use patterned lines.

Hash-based algorithms exhibit uniform distributions between the minimum and maximum chunk sizes. Rabin's Chunking (*RC*) and *TTTD* exhibit similar distributions since *TTTD* only differs from *RC* by the use of a backup divisor. *CRC* and *GEAR* exhibit similar smooth patterns as well. FastCDC (*FCDC*) is an exception, exhibiting a split pattern centered around the average chunk size. This is because it switches masks and relaxes boundary conditions past the average chunk size i.e., chunk size normalization (§II-A). *AE* and *RAM* exhibit tighter distributions when compared to hash-based algorithms.

Despite being hashless, SeqCDC exhibits a chunk size distribution similar to hash-based algorithms. We observed similar results across all our datasets and chunk sizes.

Vector acceleration. Chunk size distributions remain unaffected by vector acceleration for all CDC algorithms.

VII. ADDITIONAL RELATED WORK

Accelerating deduplication. Numerous efforts have been made to accelerate the other phases involved in data deduplication. StoreGPU [46] uses GPUs, Silo [47] uses locality-based optimizations and other work [48], [49] focuses on using faster hashing algorithms to improve fingerprint indexing. History-aware rewriting [50] and FG-DEFRAG [51] improve restore

performance by reducing fragmentation in stored chunks. HY-DRAsstor [52] and Extreme Binning [53] improve scalability by building deduplication on top of distributed storage.

While SeqCDC is compatible with many of these approaches, they are orthogonal to ours as we focus on the file chunking phase within deduplication.

Other chunking optimizations. RapidCDC [54] and QuickCDC [55] use locality-based optimizations to speed up chunking for duplicate chunks. MUCH [56] and P-Dedupe [57] parallelize chunking using multiple threads. SeqCDC is compatible with any of these techniques as they all rely on implementing optimizations on top of existing CDC algorithms.

MII [58] uses a sequence-based approach to chunk data but their approach results in inflexible chunk sizes and low throughput. Our previous work [59] discussed SeqCDC briefly. However, it does not present a methodology to accelerate SeqCDC with vector instructions or compare its performance with other vector-accelerated CDC algorithms.

Secure deduplication systems. Several efforts build end-to-end deduplication systems for encrypted data [60]. They mainly target encryption schemes [61], [62] for the underlying data or focus on reducing attacks on the system [63]. SeqCDC is compatible with all these approaches.

VIII. CONCLUSION

Deduplication systems in production employ larger chunk sizes due to reduced fingerprinting overheads. However, state-of-the-art CDC algorithms are designed to target smaller average chunk sizes, suffering from poor chunking throughput at larger sizes.

We present SeqCDC, a CDC algorithm that achieves higher chunking speeds than the state-of-the-art. SeqCDC leverages hashless lightweight boundary judgement, content-based data skipping, and SSE/AVX acceleration to improve chunking throughput by $10\times$ over unaccelerated and $1.2\times - 1.35\times$ over

vector accelerated CDC algorithms while achieving similar deduplication space savings. We hope that our work inspires a new generation of vector-friendly data chunking algorithms to accelerate data deduplication.

ACKNOWLEDGMENTS

We thank Abdelrahman Baba for his contributions to an earlier version of this paper. We thank Lori Paniak for helping us enable our experiments. This research was supported by grants from the National Cybersecurity Consortium (NCC), Natural Sciences and Engineering Research Council of Canada (NSERC) (ALLRP-561423-20 and RGPIN-2025-03332), and Acronis. Sreeharsha is supported by Ontario and Cheriton Graduate Scholarships.

APPENDIX

Table III shows the space savings achieved by all the alternatives described in §VI on all our datasets. The best performing algorithm for each dataset and chunk size combination has been highlighted using bold text. Note that there may sometimes be multiple best-performers.

SeqCDC (*SEQ*) achieves space savings within 4% of the best performer on all datasets except LNX and within 6% of the best performer on LNX.

REFERENCES

- [1] A. Holst, “Volume of data/information created, captured, copied, and consumed worldwide from 2010 to 2025,” *Statista*, June, 2021.
- [2] S. Ghemawat, H. Gobioff, and S.-T. Leung, “The Google File System,” *SIGOPS Operating Systems Review*, vol. 37, p. 29–43, oct 2003.
- [3] K. Shvachko, H. Kuang, S. Radia, and R. Chansler, “The Hadoop Distributed File System,” in *2010 IEEE 26th Symposium on Mass Storage Systems and Technologies (MSST)*, pp. 1–10, 2010.
- [4] P. M. Chen, E. K. Lee, G. A. Gibson, R. H. Katz, and D. A. Patterson, “RAID: High-performance, reliable secondary storage,” *ACM Computing Surveys (CSUR)*, vol. 26, no. 2, pp. 145–185, 1994.
- [5] G. A. Gibson and R. Van Meter, “Network attached storage architecture,” *Communications of the ACM*, vol. 43, no. 11, pp. 37–45, 2000.
- [6] D. A. Lelewer and D. S. Hirschberg, “Data compression,” *ACM Computing Surveys (CSUR)*, vol. 19, no. 3, pp. 261–296, 1987.
- [7] D. Salomon, *Data compression*. Springer, 2002.
- [8] W. Xia, H. Jiang, D. Feng, F. Douglass, P. Shilane, Y. Hua, M. Fu, Y. Zhang, and Y. Zhou, “A comprehensive study of the past, present, and future of data deduplication,” *Proceedings of the IEEE*, vol. 104, no. 9, pp. 1681–1710, 2016.
- [9] N. Mandagere, P. Zhou, M. A. Smith, and S. Uttamchandani, “Demystifying data deduplication,” in *The ACM/IFIP/USENIX Middleware’08 Conference Companion*, pp. 12–17, 2008.
- [10] D. T. Meyer and W. J. Bolosky, “A study of practical deduplication,” *ACM Transactions on Storage (ToS)*, vol. 7, no. 4, pp. 1–20, 2012.
- [11] G. Wallace, F. Douglass, H. Qian, P. Shilane, S. Smaldone, M. Channess, and W. Hsu, “Characteristics of backup workloads in production systems,” in *10th USENIX Conference on File and Storage Technologies (FAST 12)*, (San Jose, CA), USENIX Association, Feb. 2012.
- [12] L. Coyne, S. Moulton, and C. Alvarez, *IBM System Storage N Series Data Compression and Deduplication: Data ONTAP 8.1 Operating in 7-mode*. IBM Redbooks, 2012.
- [13] S. Quinlan and S. Dorward, “Venti: A New Approach to Archival Data Storage,” in *Conference on File and Storage Technologies (FAST 02)*, (Monterey, CA), USENIX Association, Jan. 2002.
- [14] Q. He, Z. Li, and X. Zhang, “Data deduplication techniques,” in *2010 international conference on future information technology and management engineering*, vol. 1, pp. 430–433, IEEE, 2010.
- [15] A. Muthitacharoen, B. Chen, and D. Mazieres, “A low-bandwidth network file system,” in *The eighteenth ACM symposium on Operating systems principles*, pp. 174–187, 2001.

Dataset	CDC	4KB	8KB	16KB
DEB	AE	41.99%	33.69%	21.94%
	CRC	41.65%	35.23%	26.59%
	FCDC	43.83%	36.10%	26.47%
	GEAR	39.49%	33.12%	24.12%
	RC	44.38%	36.16%	27.22%
	RAM	42.98%	34.21%	22.37%
	TTTD	45.06%	37.13%	27.94%
DEV	SEQ	42.77%	37.76%	29.67%
	AE	98.00%	97.75%	97.21%
	CRC	98.15%	98.09%	97.98%
	FCDC	98.17%	98.06%	97.90%
	GEAR	98.14%	98.07%	97.98%
	RC	98.21%	98.12%	97.97%
	RAM	98.05%	97.79%	97.31%
LNX	TTTD	98.22%	98.12%	97.98%
	SEQ	98.13%	98.03%	97.82%
	AE	59.41%	45.35%	31.67%
	CRC	62.43%	48.70%	36.01%
	FCDC	59.16%	43.92%	33.64%
	GEAR	57.80%	40.94%	28.93%
	RC	67.02%	50.90%	35.40%
RDS	RAM	57.94%	45.62%	29.12%
	TTTD	68.46%	51.06%	36.92%
	SEQ	63.13%	49.46%	33.26%
	AE	94.66%	92.94%	91.04%
	CRC	94.66%	93.72%	92.02%
	FCDC	93.82%	92.17%	90.15%
	GEAR	92.44%	93.01%	89.92%
TPCC	RC	94.31%	92.27%	90.57%
	RAM	95.67%	94.09%	92.03%
	TTTD	95.2%	92.80%	91.55%
	SEQ	94.86%	92.54%	88.78%
	AE	86.58%	84.96%	81.58%
	CRC	87.23%	86.79%	86.40%
	FCDC	87.18%	86.74%	86.17%
TPCC	GEAR	86.96%	86.64%	86.36%
	RC	87.24%	86.80%	86.37%
	RAM	86.71%	85.21%	81.67%
	TTTD	87.29%	86.84%	86.40%
	SEQ	87.04%	86.68%	85.83%

TABLE III: Space savings of CDC techniques. Note that the best algorithm at each configuration is shown using bold text and that *SEQ* is native (unaccelerated) SeqCDC.

- [16] J. Kubiawicz, D. Bindel, Y. Chen, S. Czerwinski, P. Eaton, D. Geels, R. Gummadi, S. Rhea, H. Weatherspoon, W. Weimer, *et al.*, “Oceanstore: An architecture for global-scale persistent storage,” *ACM SIGOPS Operating Systems Review*, vol. 34, no. 5, pp. 190–201, 2000.
- [17] Y. Zhang, H. Jiang, D. Feng, W. Xia, M. Fu, F. Huang, and Y. Zhou, “AE: An asymmetric extremum content defined chunking algorithm for fast and bandwidth-efficient data deduplication,” in *2015 IEEE Conference on Computer Communications (INFOCOM)*, pp. 1337–1345, IEEE, 2015.
- [18] F. Ni, X. Lin, and S. Jiang, “SS-CDC: a two-stage parallel content-defined chunking for deduplicating backup storage,” in *Proceedings of the 12th ACM International Conference on Systems and Storage, SYSTOR ’19*, (New York, NY, USA), p. 86–96, Association for Computing

- Machinery, 2019.
- [19] W. Xia, Y. Zhou, H. Jiang, D. Feng, Y. Hua, Y. Hu, Q. Liu, and Y. Zhang, "FastCDC: A fast and efficient content-defined chunking approach for data deduplication," in *2016 USENIX Annual Technical Conference (USENIX ATC 16)*, pp. 101–114, 2016.
 - [20] W. Xia, H. Jiang, D. Feng, L. Tian, M. Fu, and Y. Zhou, "Ddelta: A deduplication-inspired fast delta compression approach," *Performance Evaluation*, vol. 79, pp. 258–272, 2014. Special Issue: Performance 2014.
 - [21] R. N. Widodo, H. Lim, and M. Atiquzzaman, "A new content-defined chunking algorithm for data deduplication in cloud storage," *Future Generation Computer Systems*, vol. 71, pp. 145–156, 2017.
 - [22] K. Eshghi and H. K. Tang, "A framework for analyzing and improving content-based chunking algorithms," *Hewlett-Packard Labs Technical Report TR*, vol. 30, no. 2005, 2005.
 - [23] N. Bjørner, A. Blass, and Y. Gurevich, "Content-dependent chunking for differential compression, the local maximum approach," *Journal of Computer and System Sciences*, vol. 76, no. 3–4, pp. 154–203, 2010.
 - [24] A. W. Appel, "Verification of a cryptographic primitive: SHA-256," *ACM Transactions on Programming Languages and Systems (TOPLAS)*, vol. 37, no. 2, pp. 1–31, 2015.
 - [25] S. Udayashankar, A. Baba, and S. Al-Kiswany, "VectorCDC: Accelerating Data Deduplication with Vector Instructions," in *USENIX Conference on File and Storage Technologies*, 2025.
 - [26] J. E. Smith, G. Faanes, and R. Sugumar, "Vector instruction set support for conditional operations," *ACM SIGARCH Computer Architecture News*, vol. 28, no. 2, pp. 260–269, 2000.
 - [27] A. Liu, A. Baba, S. Udayashankar, and S. Al-Kiswany, "Dedup-bench: A Benchmarking Tool for Data Chunking Techniques," in *2023 IEEE Canadian Conference on Electrical and Computer Engineering (CCECE)*, pp. 469–474, 2023.
 - [28] R. L. Rivest, "The MD5 Message-Digest Algorithm." RFC 1321, 1992.
 - [29] M. A. Jarah, S. Udayashankar, A. Baba, and S. Al-Kiswany, "The Impact of Low-Entropy on Chunking Techniques for Data Deduplication," in *2024 IEEE 17th International Conference on Cloud Computing (CLOUD)*, pp. 134–140, 2024.
 - [30] S. A. Hassan, M. M. Mahmoud, A. Hemeida, and M. A. Saber, "Effective implementation of matrix-vector multiplication on intel's avx multicore processor," *Computer Languages, Systems & Structures*, vol. 51, pp. 158–175, 2018.
 - [31] S. Gueron and V. Krasnov, "Fast quicksort implementation using AVX instructions," *The Computer Journal*, vol. 59, no. 1, pp. 83–90, 2016.
 - [32] R. L. Bocchino Jr and V. S. Adve, "Vector LLVA: a virtual vector instruction set for media processing," in *Proceedings of the 2nd international conference on Virtual execution environments*, pp. 46–56, 2006.
 - [33] T.-S. Moh and B. Chang, "A running time improvement for the two thresholds two divisors algorithm," in *The 48th Annual Southeast Regional Conference*, pp. 1–6, 2010.
 - [34] Intel, "Intel® Intrinsics Guide." <https://www.intel.com/content/www/us/en/docs/intrinsics-guide/index.html>.
 - [35] C. Z. Mooney, *Monte carlo simulation*. Sage, 1997.
 - [36] VMWare, "VMWare marketplace." <https://marketplace.cloud.vmware.com/services>, 2023.
 - [37] Rust, "GitHub - rust-lang/rust: Empowering everyone to build reliable and efficient software." <https://github.com/rust-lang/rust>, 2023.
 - [38] Linux, "The Linux Kernel Archives." <https://www.kernel.org/>, 2023.
 - [39] Redis, "Redis." <https://redis.io/>, 2023.
 - [40] MySQL, "MySQL." <https://www.mysql.com/>, 2023.
 - [41] T. P. Council, "TPC-C Overview." <https://www.tpc.org/tpcc/detail5.asp>, 2023.
 - [42] D. Duplyakin, R. Ricci, A. Maricq, G. Wong, J. Duerig, E. Eide, L. Stoller, M. Hibler, D. Johnson, K. Webb, A. Akella, K. Wang, G. Ricart, L. Landweber, C. Elliott, M. Zink, E. Cecchet, S. Kar, and P. Mishra, "The Design and Operation of CloudLab," in *2019 USENIX Annual Technical Conference (USENIX ATC 19)*, (Renton, WA), pp. 1–14, USENIX Association, July 2019.
 - [43] S. Udayashankar, A. Baba, and S. Al-Kiswany, "VM Images for Deduplication." <https://www.kaggle.com/dsv/10561721>, 2025.
 - [44] D. Kanter, "Intel's Haswell CPU microarchitecture," *Real World Technologies*, vol. 17, 2012.
 - [45] M. Gottschlag, T. Schmidt, and F. Bellosa, "AVX overhead profiling: How much does your fast code slow you down?," in *Proceedings of the 11th ACM SIGOPS Asia-Pacific Workshop on Systems*, APSys '20, (New York, NY, USA), p. 59–66, Association for Computing Machinery, 2020.
 - [46] S. Al-Kiswany, A. Gharaibeh, E. Santos-Neto, G. Yuan, and M. Rippeanu, "StoreGPU: Exploiting Graphics Processing Units to Accelerate Distributed Storage Systems," in *The 17th International Symposium on High Performance Distributed Computing*, HPDC '08, (New York, NY, USA), p. 165–174, Association for Computing Machinery, 2008.
 - [47] W. Xia, H. Jiang, D. Feng, and Y. Hua, "Similarity and Locality Based Indexing for High Performance Data Deduplication," *IEEE Transactions on Computers*, vol. 64, no. 4, pp. 1162–1176, 2015.
 - [48] J. Li, Z. Yang, Y. Ren, P. P. Lee, and X. Zhang, "Balancing storage efficiency and data confidentiality with tunable encrypted deduplication," in *Proceedings of the Fifteenth European Conference on Computer Systems*, pp. 1–15, 2020.
 - [49] C. Song, X. Chen, D. Liu, J. Li, Y. Tan, and A. Ren, "Optimizing the Performance of Consistency-Aware Deduplication Using Persistent Memory," *IEEE Transactions on Computer-Aided Design of Integrated Circuits and Systems*, 2023.
 - [50] M. Fu, D. Feng, Y. Hua, X. He, Z. Chen, W. Xia, F. Huang, and Q. Liu, "Accelerating restore and garbage collection in deduplication-based backup systems via exploiting historical information," in *2014 USENIX Annual Technical Conference (USENIX ATC 14)*, (Philadelphia, PA), pp. 181–192, USENIX Association, June 2014.
 - [51] Y. Tan, B. Wang, J. Wen, Z. Yan, H. Jiang, and W. Srisa-an, "Improving Restore Performance in Deduplication-Based Backup Systems via a Fine-Grained Defragmentation Approach," *IEEE Transactions on Parallel and Distributed Systems*, vol. 29, no. 10, pp. 2254–2267, 2018.
 - [52] C. Dubnicki, L. Gryz, L. Heldt, M. Kaczmarczyk, W. Kilian, P. Strzelczak, J. Szczepkowski, C. Ungureanu, and M. Welnicki, "HYDRAsTOR: A scalable secondary storage," in *FAST*, vol. 9, pp. 197–210, 2009.
 - [53] D. Bhagwat, K. Eshghi, D. D. E. Long, and M. Lillibridge, "Extreme Binning: Scalable, parallel deduplication for chunk-based file backup," in *2009 IEEE International Symposium on Modeling, Analysis and Simulation of Computer and Telecommunication Systems*, pp. 1–9, 2009.
 - [54] F. Ni and S. Jiang, "RapidCDC: Leveraging Duplicate Locality to Accelerate Chunking in CDC-Based deduplication systems," in *The ACM Symposium on Cloud Computing*, SoCC '19, (New York, NY, USA), p. 220–232, Association for Computing Machinery, 2019.
 - [55] Z. Xu and W. Zhang, "QuickCDC: A Quick Content Defined Chunking Algorithm Based on Jumping and Dynamically Adjusting Mask Bits," in *2021 IEEE Intl Conf on Parallel & Distributed Processing with Applications, Big Data & Cloud Computing, Sustainable Computing & Communications, Social Computing & Networking (ISPA/BDCloud/SocialCom/SustainCom)*, pp. 288–299, 2021.
 - [56] Y. Won, K. Lim, and J. Min, "MUCH: Multithreaded Content-Based File Chunking," *IEEE Transactions on Computers*, vol. 64, no. 5, pp. 1375–1388, 2015.
 - [57] W. Xia, H. Jiang, D. Feng, L. Tian, M. Fu, and Z. Wang, "P-dedupe: Exploiting parallelism in data deduplication system," in *2012 IEEE Seventh International Conference on Networking, Architecture, and Storage*, pp. 338–347, IEEE, 2012.
 - [58] C. Zhang, D. Qi, Z. Cai, W. Huang, X. Wang, W. Li, and J. Guo, "MII: A Novel Content Defined Chunking Algorithm for Finding Incremental Data in Data Synchronization," *IEEE Access*, vol. 7, pp. 86932–86945, 2019.
 - [59] S. Udayashankar, A. Baba, and S. Al-Kiswany, "SeqCDC: Hashless Content-Defined Chunking for Data Deduplication," in *Proceedings of the 25th International Middleware Conference*, Middleware '24, (New York, NY, USA), p. 292–298, Association for Computing Machinery, 2024.
 - [60] Y. Shin, D. Koo, and J. Hur, "A Survey of Secure Data Deduplication Schemes for Cloud Storage Systems," *ACM Computing Surveys*, vol. 49, Jan 2017.
 - [61] M. Bellare, S. Keelveedhi, and T. Ristenpart, "Message-locked encryption and secure deduplication," in *Annual international conference on the theory and applications of cryptographic techniques*, pp. 296–312, Springer, 2013.
 - [62] J. Liu, N. Asokan, and B. Pinkas, "Secure Deduplication of Encrypted Data without Additional Independent Servers," in *Proceedings of the 22nd ACM SIGSAC Conference on Computer and Communications Security*, CCS '15, (New York, NY, USA), p. 874–885, Association for Computing Machinery, 2015.
 - [63] D. Harnik, B. Pinkas, and A. Shulman-Peleg, "Side Channels in Cloud Services: Deduplication in Cloud Storage," *IEEE Security and Privacy*, vol. 8, no. 6, pp. 40–47, 2010.